

# Spatiotemporal noise covariance model for MEG/EEG data source analysis

S.M. P. Lis    J.S. George    S.C. Jun    J. Pare-Balaguer  
D.M. Ranken    D.M. Schmidt    C.C. Wood

## Abstract

A new method for approximating spatiotemporal noise covariance for use in MEG/EEG source analysis is proposed. Our proposed approach extends a parameterized one pair approximation consisting of a Kronecker product of a temporal covariance and a spatial covariance [1] into 1) an unparameterized one pair approximation and then 2) into a multipair approximation. These models are motivated by the need to better describe correlated background and make estimation of these models more efficient. The effects of these different noise covariance models are compared using a multi-dipole inverse algorithm and simulated data consisting of empirical MEG background data as noise and simulated dipole sources.

## Index Terms

MEG, EEG, Spatiotemporal Analysis, Noise Modelling, Inverse Problem.

## I. Introduction

The magnetoencephalogram (MEG)/electroencephalogram (EEG) source localization problem is to infer active brain regions from measurements outside of the human head. Often, for example in evoked response experiments, the data from individual stimulus trials are averaged, time-locked to the stimulus presentation. This averaged post-stimulus data (signal) is compared with the statistical properties of the averaged data far from the stimulus (representing background) and this difference is used to infer the location and time-courses of neural activity that were, at least on average, generated in response to the given stimulus. Because these inferences are based on differences between signal and background, it is important to characterize the background as accurately as possible. This is especially important in spatiotemporal analysis since background is correlated both in space and time.

The log likelihood function is a common mathematical expression quantifying the likelihood of a given model (current distribution) matching the data. For Gaussian zero-mean noise background spatiotemporal data log likelihood is given by:

$$\frac{1}{2} \sum_{k,t} \mathbf{b}_{k,t}^T \text{COV}^{-1}_{k,t;k_0,t_0} \mathbf{b}_{k_0,t_0} - \sum_{k,t} \mathbf{L}_k(\mathbf{x})^T \mathbf{j}(\mathbf{x};t) \mathbf{dx} \quad (1)$$

Here  $\mathbf{b}_{k,t}$  are the measurements (the data being analyzed) at sensor  $k$  and time  $t$ ,  $\mathbf{L}_k(\mathbf{x})$  is the lead field at point  $\mathbf{x}$  for the sensor  $k$ ,  $\mathbf{j}(\mathbf{x};t)$  is the current distribution function used in the forward model and  $\text{COV}$  is averaged background (assumed to be Gaussian) covariance, which describes second order statistical properties of MEG/EEG background in time and space. There are a number of different inverse algorithms in use [2-7] but most use the likelihood formulation in some way. In all cases, accurate covariance is required to solve source localization problem more accurately. However,

the covariance has been commonly taken to be diagonal, even though there is ample evidence that the background averaged data is correlated within both space and time [8,10]. This may affect the results of inverse calculations, such as biasing source location [11], as is demonstrated here.

In principle, if a normal distribution is assumed, the full covariance matrix of the averaged data can be estimated in the following way. MEG/EEG is measured in  $M$  trials, on  $L$  sensors and in  $C$  time samples. Let  $E_m$  be the  $L$  by  $C$  single trial noise matrix at trial  $m$ . Conventionally, the full averaged noise covariance matrix of dimension  $N = LC$  is estimated by

$$COV = \frac{1}{M} \sum_{m=1}^M (\text{vec}(E_m) - \text{vec}(E)) (\text{vec}(E_m) - \text{vec}(E))^T; \quad (2)$$

$$E = \frac{1}{M} \sum_{m=1}^M E_m \quad (3)$$

where  $\text{vec}(E)$  is all the columns of  $E$  stacked in a vector.

There are a number of reasons why this estimate of the full covariance is difficult to use and why an adequate approximation is needed. First, sufficient experimental data is rarely available to adequately estimate the large number of parameters present in the full covariance matrix for modern multi-sensor setups. For example, for 35 time samples and 121 channels and considering the fact that covariance matrix is symmetric, 8,969,730 parameters should be determined. Second, since spatiotemporal noise covariance matrix in this form is extremely large, a tremendous amount of memory is required for its storage. Third, this full covariance is almost impossible to handle in the likelihood formulation, since computation time of calculating the inverse still renders the task infeasible in most interesting cases. A naive algorithm for matrix inversion takes  $O(N^3)$  time and though there are some improvements over this result for large matrices [12,13], it is still hard with any interesting  $N$ . Here,  $N$  is the dimensionality of the matrix. Due to all these difficulties with the estimate of the full spatiotemporal covariance, some approximation needs to be introduced.

## II. Models

In this section we describe several models approximating the full spatiotemporal noise covariance. Among them are two existing models and three models we introduce in this paper. Existing models include the widely used diagonal approximation and a Kronecker product approximation introduced by Huizenga et al [1]. We introduce two additional models based on a single Kronecker product approximation. They are: an unparameterized maximum likelihood approximation and one pair model calculated from the data. And most important, we present a new multi-pair model based on a series of Kronecker products. Three of these five models are compared later in the paper. They are: diagonal approximation, one pair model calculated from the data and multi-pair approximation.

### A. Diagonal approximation

It is common when solving the inverse problem to model covariance as a diagonal or even just as an identity. In this case the full spatiotemporal covariance is  $COV = T^{-1} S$ , where  $T$  is the temporal covariance which is taken to be identity and  $S$  is the diagonal spatial covariance with elements of the main diagonal being sensor variances. This model is very simple and yet still generates noise with variance levels consistent with those of noise generated by more complex models described below.

B. Kronecker product approximation

B.1 An existing model

As an improvement over the widely used, generic diagonal approximation, Huizenga et al. proposed a Kronecker product of a C by C temporal covariance matrix T and a L by L spatial covariance matrix S [1,14], where C is the number of time samples and L is the number of sensors:

$$COV_{T,S} = \begin{bmatrix} T_{11}S & T_{12}S & \dots & T_{1C}S \\ T_{21}S & T_{22}S & \dots & T_{2C}S \\ \vdots & \vdots & \ddots & \vdots \\ T_{C1}S & T_{C2}S & \dots & T_{CC}S \end{bmatrix} \quad (4)$$

To reduce the number of free parameters in the model both spatial and temporal covariances were parameterized. It was assumed that spatial covariance can be modeled as an exponential function of the distance between sensors [1]:

$$S_{ll^0} = \hat{\sigma}_1 \hat{\sigma}_{l^0} \exp(-d_{ll^0} / \hat{\lambda}) \quad (5)$$

where  $d_{ll^0}$  is the distance between sensors l and  $l^0$ ,  $\hat{\sigma}_1$  and  $\hat{\sigma}_{l^0}$  are the standard deviations of corresponding sensors, and  $\hat{\lambda}$  and  $\hat{\lambda}^0$  are free parameters. In this model, covariance between sample t and  $t^0$  was denoted as a scalar  $T_{tt^0}$  and it was assumed that temporal covariances are only dependent on the lag  $t - t^0$  between samples. It follows that temporal covariance could be expressed as Toeplitz matrix.

Huizenga et al. also assumed that the full covariance matrix has been estimated. They suggested two ways to determine the parameters to their Kronecker model. First, by minimizing:

$$\text{tr} \{ F^{-1} \hat{T}^{-1} \hat{S}^{-1} W^{-1} g \} \quad (6)$$

where F is the full spatiotemporal covariance (2) and  $\hat{T}$  and  $\hat{S}$  are estimates of T and S, respectively. Note that W is the weighting matrix and setting it to different values gives different noise parameter estimates. For example setting it to I yields Ordinary Least Squares (OLS) estimate. Second, by minimizing [1,15]:

$$(\hat{T}; \hat{S}) = \ln \{ \hat{T}^{-1} \hat{S}^{-1} \} + \text{tr} \{ \hat{T}^{-1} \hat{S}^{-1} F g \} = L \ln \{ \hat{T}^{-1} \} + C \ln \{ \hat{S}^{-1} \} + \text{tr} \{ \hat{T}^{-1} \hat{S}^{-1} F \} \quad (7)$$

which gives Maximum Likelihood (ML) covariance estimate. Inversion of this model is easily calculated by using the following identity:

$$[T^{-1} S^{-1}] = T^{-1} S^{-1} \quad (8)$$

However, the Huizenga model was found unworkable for our dataset, described below. The most important difficulty we encountered working with this model was numerical instability, which led to the impossibility of inverting the spatial and temporal covariances because they were numerically almost singular. This was likely due to their parameterization of spatial covariance (5):  $\hat{\lambda}$  in the denominator of a fraction which is an argument to exponential function was contributing to forming a numerically unstable matrix. These difficulties lead us to introduce other models based on this one so it would be possible to use it for comparison purposes.

B.2 Unparam eterized maximum likelihood model

In order to have a one Kronecker product model for subsequent comparisons that would work in our case we introduce another model. In this model, both spatial and temporal covariances are unparam eterized leading to several benefits. Importantly it is not prone to numerical instability – solutions in our analysis had numerically tractable inverses. Also, the increased number of free parameters allows the proposed model to capture more information about the noise than Huizenga’s (see section B.1). Finally, this model is markedly faster in the convergence of iterative fitting of the model to the full spatiotemporal covariance because an analytical calculation of partial derivatives of (7) is possible (see appendix A). Having obtained partial derivatives of  $\ln \mathcal{L}(\hat{T}; \hat{S})$ , namely  $\frac{\partial \ln \mathcal{L}(\hat{T}; \hat{S})}{\partial \hat{T}^{-1}}$  and  $\frac{\partial \ln \mathcal{L}(\hat{T}; \hat{S})}{\partial \hat{S}^{-1}}$ , it is easy to devise an iterative algorithm for minimizing  $\ln \mathcal{L}(\hat{T}; \hat{S})$ . This derivative basically yields the same results as [14].

Note that this estimate can give sensor variances inconsistent with those estimated from the data and given by other models (see for example figure 1). This is expected as we are obtaining

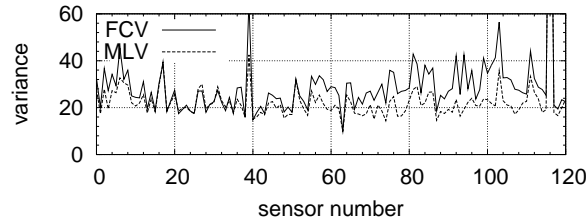


Fig.1. Sensor variances estimated by the full spatiotemporal covariance (FCV) defined in (2) and by unparam eterized maximum likelihood model estimate (MLV).

Maximum Likelihood estimates without constraining our model to keep correct variances. That is, maximizing the likelihood does not necessarily mean keeping sensor variances consistent with those that are correct. Below we explain our solution to this issue.

B.3 One pair model calculated from the data

To overcome this feature, and observing that the model  $T \otimes S$  assumes independence between space and time, we can estimate  $T$  and  $S$  directly from the data by:

$$\hat{T} = \frac{1}{M(LM - 1)} \begin{pmatrix} E_1^T & \dots & E_M^T \\ B & & C \\ 0 & E_1 & 1 \\ & \vdots & A \end{pmatrix} \quad (9)$$

$$\hat{S} = \frac{1}{M(CM - 1)} \begin{pmatrix} E_1 & \dots & E_M \\ B & & C \\ 0 & E_1^T & 1 \\ & \vdots & A \\ & & & E_M^T \end{pmatrix} \quad (10)$$

where  $E_m$  is a  $L \times C$  single trial noise data with  $L$  number of sensors and  $C$  number of time points,  $M$  is number of trials. The above is true with the assumption that each sensor measurement, at any time point, at any epoch, is an independent and identically distributed (i.i.d.) random vector; and each time vector for any sensor at any epoch is also an i.i.d. random vector. Correctness of this estimation for the model can be demonstrated if we assume that the noise was indeed generated

from this model. For more details of this argument see appendix B. Inherently, this model yields the same sensor variances as the full covariance.

We use this modified version of the one pair Huizenga model for comparisons with the diagonal model and our multipair model in the rest of the paper.

### C. Multipair approximation

In an attempt to capture more properties of the full covariance while still allowing for inversion we propose an alternative estimation of noise covariance as a series of Kronecker products of temporal covariance matrices  $T^l$  and orthogonal spatial covariance matrices  $S^l$  expressed as:

$$COV = \prod_{l=1}^L T^l S^l \tag{11}$$

Assuming that we have  $M$  times single trial noise data, singular value decomposition is applied to background noise data  $A$ :

$$A = \begin{bmatrix} 0 & E_1^T & 1 \\ \vdots & E_2^T & \vdots \\ E_m^T & \vdots & A \\ \vdots & \vdots & \vdots \\ E_M^T & \vdots & A \end{bmatrix} = U \begin{bmatrix} 0 & U_1 & 1 \\ \vdots & U_2 & \vdots \\ U_m & \vdots & A \\ \vdots & \vdots & \vdots \\ U_M & \vdots & A \end{bmatrix} V^T \tag{12}$$

where  $V$  is an  $L \times L$  orthogonal matrix of spatial components, the  $U_i$  form a  $CM \times L$  orthogonal matrix  $U$  of initial time courses rotated into the spacial orthogonal space, and  $A$  is an  $L \times L$  diagonal matrix with  $\lambda_{ii}$  being singular values of  $A$ . By the above matrix formulation,

$$E_m^T = U_m V^T$$

and by averaging over  $M$  trials, we denote

$$E^T = \frac{1}{M} \sum_m E_m^T = \frac{1}{M} \sum_m U_m V^T = U V^T :$$

#### C.1 Relationship to full covariance

The spatiotemporal covariance estimate (2) can be reformulated in the following way:

$$\frac{1}{M(M-1)} \sum_m \begin{bmatrix} (E_m E)_1 \\ \vdots \\ (E_m E)_t \\ \vdots \\ (E_m E)_c \end{bmatrix} \begin{bmatrix} 1 \\ \vdots \\ A \\ \vdots \\ A \end{bmatrix} = \begin{bmatrix} B_{11} & & & \\ & \ddots & & \\ & & B_{tt^0} & \\ & & & \ddots \\ B_{c1} & & & & B_c \end{bmatrix}$$

In the above, the  $t^{\text{th}}$  column of  $E_m - E$  is denoted by  $(E_m - E)_t$ . These columns represent sensor measurements at time  $t$ . The  $B_{t,t^0}$  are blocks of a block matrix each of which is  $\frac{1}{M(M-1)} (E_m - E)_t [(E_m - E)_{t^0}]^T$ : Since  $(E_m - E)^T = (U_m - U) V^T$ ;

$$\frac{1}{M(M-1)} \sum_m (E_m - E)_t [(E_m - E)_{t^0}]^T = V^{-T} T_{t,t^0} V^T$$

Here,  $T_{t,t^0} = \frac{1}{M(M-1)} \sum_m [(U_m - U)^T]_t [(U_m - U)^T]_{t^0}^T$ , which can be represented in the following way:

$$T_{t,t^0} = \frac{1}{M(M-1)} \sum_m \begin{pmatrix} 0 & u_{m,t}^1 & u_t^1 & 1 \\ u_{m,t}^2 & u_t^2 & C & \\ \vdots & \vdots & C & \\ u_{m,t}^L & u_t^L & A & u_{m,t^0}^1 & u_{t^0}^1 & u_{m,t^0}^2 & u_{t^0}^2 & \vdots & u_{m,t^0}^L & u_{t^0}^L \\ 0 & (u_{m,t}^1 & u_t^1) & (u_{m,t^0}^1 & u_{t^0}^1) & (u_{m,t}^1 & u_t^1) & (u_{m,t^0}^2 & u_{t^0}^2) & 1 \\ B & (u_{m,t}^2 & u_t^2) & (u_{m,t^0}^1 & u_{t^0}^1) & (u_{m,t}^2 & u_t^2) & (u_{m,t^0}^2 & u_{t^0}^2) & C \\ \vdots & \vdots & \vdots & \vdots & \ddots & \vdots & \vdots & \vdots & \vdots & A \end{pmatrix}$$

Diagonal entries of this matrix are time-lagged autocovariances, and off-diagonal entries ( $l;l^0$ ) are cross covariances between (time  $t$ , component  $l$ ) and (time  $t^0$ , component  $l^0$ ). Assuming cross covariances of spatiotemporal data are negligibly small, i.e. that  $T_{t,t^0}$  is an almost diagonal matrix, we obtain the following equation:

$$\begin{aligned} \frac{1}{M(M-1)} \sum_m (E_m - E)_t [(E_m - E)_{t^0}]^T &= V^{-T} T_{t,t^0} V^T \\ &= \sum_{l=1}^{X^L} \frac{1}{2} T_{t,t^0}^{l;l} V_1 V_1^T + \sum_{l^0=1}^X \frac{1}{2} T_{t,t^0}^{l;l^0} V_1 V_{l^0}^T \\ &= \sum_{l=1}^{X^L} \frac{1}{2} T_{t,t^0}^{l;l} S^1 + \sum_{l^0=1}^X \frac{1}{2} T_{t,t^0}^{l;l^0} V_1 V_{l^0}^T \\ &= \sum_{l=1}^{X^L} \frac{1}{2} T_{t,t^0}^{l;l} S^1 \end{aligned}$$

Here,  $S^1 = V_1 V_1^T$ , and

$$T_{t,t^0}^{l;l} = \frac{1}{M(M-1)} \sum_{m=1}^M (u_{m,t}^l - u_t^l) (u_{m,t^0}^l - u_{t^0}^l)$$

Note that the above assumption of small cross covariances lets us construct a model which is easily invertible due to the orthogonality of spatial components. In cases where this assumption does not hold, the model might not perform optimally.

C.2 Properties of Multipair Model

Our Multipair Model is

$$COV = \sum_{l=1}^{X^L} T_l^{-1} S_l^1;$$

where  $S_l^1$  are constructed from the orthogonal singular vectors of the SVD of the data and  $T_l^{-1}$  are constructed from the data having been rotated into the orthogonal space formed by spatial components. This model has less free parameters than the full spatiotemporal covariance estimate (2) and has more expressive power than the one Kronecker product model (4) described in [1]. A very important feature that favorably distinguishes this model is that it does not need the full spatiotemporal covariance and can be estimated directly from the data. Also, inversion is still computationally manageable and only a constant time slower than inversion of (4).

Proposition 1: The inversion of  $COV$  can be expressed by

$$COV^{-1} = \sum_{l=1}^{X^L} T_l^{-2} (T_l^{-1})^{-1} S_l^1;$$

Proof. By the identity  $(A_1 \ B_1)(A_2 \ B_2) = (A_1 A_2 \ B_1 B_2)$  and the orthogonality of  $S^1$  ( $S^1 S^1 = 0$  if  $l \neq l'$ ),

$$\begin{aligned} & \sum_{l=1}^{X^L} T_l^{-2} S_l^1 \sum_{l'=1}^{X^L} T_{l'}^{-2} (T_{l'}^{-1})^{-1} S_{l'}^1 \\ &= \sum_{l=1}^{X^L} I (S_l^1)^2 \end{aligned}$$

By two properties of  $S^1$ : (1)  $(S^1)^2 = S^1$ ; (2)  $\sum_{l=1}^P S_l^1 = I$  due to orthogonality of  $V$ , we obtain the desired one:

$$\sum_{l=1}^{X^L} I (S_l^1)^2 = \sum_{l=1}^{X^L} S_l^1 = I \quad I = I;$$

III. Comparison of covariance models

Empirical MEG data used for comparing these noise covariance models were acquired in the following experiment:

Median nerve stimulation at the motor twitch threshold was applied using a block design of 30s on, 30s off for a total of 10 blocks for each of 8 runs. The stimulus alternated across runs, with four runs total of left side stimulation and four runs total of right side stimulation. The ISI (interstimulus interval) was randomized from between 0.25 and 0.75s (Fig. 2). Such setup provides for easier collection of brain noise since there is no stim for long periods. This feature might be useful in other noise studies. Data were collected on 4D Neuroimaging Neuromag-122 whole-head gradiometer system with 122 channels [16]. The experiment used a male subject, age 38, sampling rate was set to 1000Hz.

A median filter was chosen because high-pass filtering was introducing substantial distortions to the signal in the averaged data. These distortions expressed themselves more strongly as the cutoff frequency values increased. In figure 3, comparisons are shown between changes introduced by a high-pass filter for 10Hz (3(b)) and the much smaller changes that appeared after median filtering

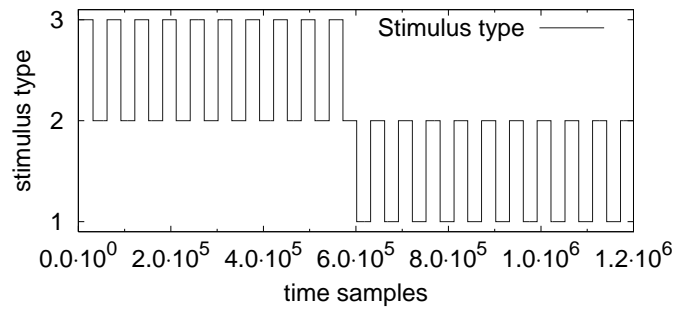


Fig. 2. The manner in which stimuli were applied in the experiment. x-axis shows time samples and y-axis – stimulus types, where type 1 – right hand, 2 – no stimulus, 3 – left hand.

(3 (c)). The original, unfiltered signal is also presented for reference (3 (a)). The value of 10 Hz was chosen since at this cutoff, distortions are clearly seen. In this paper, a 1 Hz cutoff frequency was used. Distortions introduced by a high-pass filter are not as evident there but should still be bigger than those introduced by subtracting the median filtered signal from the original signal for the high pass effect. This justifies the use of median filtering.

The 60 Hz noise and harmonics were handled by removing peaks in the spectrum and then interpolating between adjacent spectrum points.

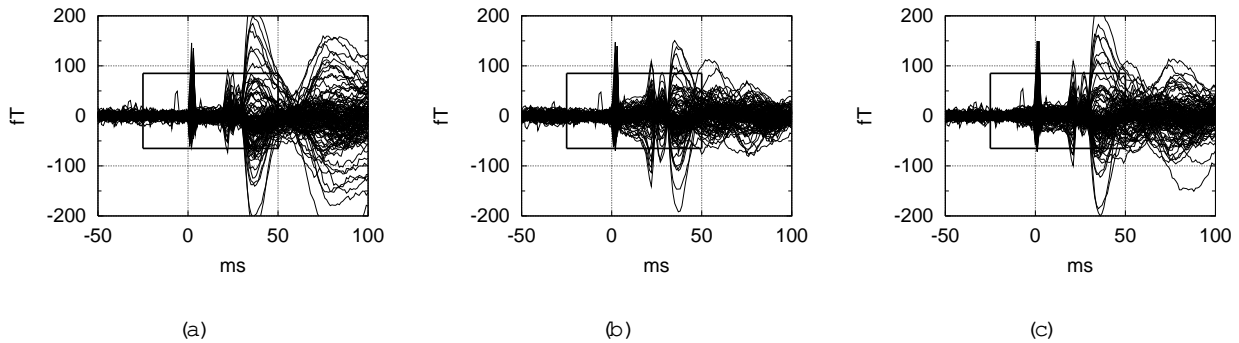


Fig. 3. Filtering choices for the data used in this paper: (a) no filtering used; (b) a highpass filter for 10 Hz is used; (c) data subtracted a median filtered data for 10 Hz high pass effect. The rectangles indicate the region where the distortions introduced by filtering are most noticeable.

#### A. Comparing model covariances to full covariance

We compare three models described in the previous section in terms of their ability to approximate the full spatiotemporal covariance and also in terms of the performance of an inverse algorithm employing those models. These models are: diagonal approximation, one pair model calculated from the data and the multipair model. We have used 121 channel data with 35 time points (35 ms with the used sampling frequency). This time interval is the maximal interval at which we still had enough data samples available for reliable estimation of the full spatiotemporal covariance matrix. Estimation of the full spatiotemporal covariance matrix is needed since it is used for comparisons. Channel 51 was removed due to the presence of a large number of artifacts. Covariance models were calculated using the formulation in the previous section. All covariances were consistent with each other in that they yielded the same sensor variances. The only difference was in the correlation

structure.

In figure 4, scatterplots of spatiotemporal covariance approximation models with the full covariance are plotted. These plots were constructed by plotting points on a graph such that the x-coordinate of a point is the value of an element of the full spatiotemporal covariance and the y-coordinate is the value of the corresponding element in the model covariance. Distribution was scaled to the same range of values. Such a construction provides information about structural correspondence of the models with the full covariance. The case of ideal coincidence should give a figure with all points located along a line that goes through the origin and forms a 45° angle with the x-axis. In order to have a reference each figure is plotted over a figure that has a point for each element of the full spatiotemporal covariance with x and y coordinates equal to each other and equal to the value of this element. Even though it is clear that all points of this figure will be located on a 45° line, this still gives additional information about which values are present in the covariance. In the case when the approximation is very close to the full covariance, the scatterplot should be very close to this reference plot. Note that the scatterplot of the diagonal approximation and the full spatiotemporal covariance (shown in 4(a)) is very different from the other two. Many points of this plot are on the x-axis. This is easily explained by an observation that non-zero off-diagonal elements of the full spatiotemporal covariance correspond to zero off-diagonal elements of the diagonal approximation. This means that for each off-diagonal element of the full spatiotemporal covariance we place a point with the corresponding x-coordinate and the zero y-coordinate. These figures suggest that our proposed multipair spatiotemporal covariance model should be better than the other two models in approximating the structure of the full spatiotemporal covariance.

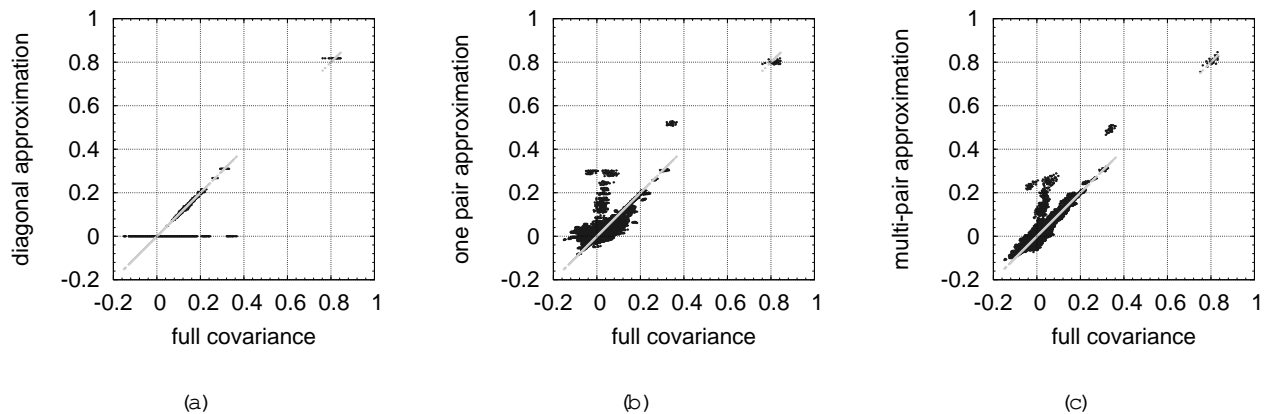


Fig. 4. Scatterplots of spatiotemporal covariance approximation models with the full covariance: (a) diagonal approximation; (b) one pair approximation estimated from the data; (c) multipair approximation.

## B. Comparing noise models in an inverse algorithm

In order to compare performance of the models in an inverse algorithm, we used simulated data constructed with three dipoles acting in the region of 35ms using the same physical setup as in the empirical experiment. Locations are given on a sphere fitted to the skull with the z axis pointing up, the y axis pointing left and the x axis pointing forward. Dipole parameters are presented in Table I.

To these simulated dipoles, we added noise extracted from prestimulus regions of type 1 stimulus

TABLE I  
Parameters of simulated dipoles

number	location (mm)	moment	max strength (nAm)
1	(0,0,30)	(1,0,0)	50
2	(-30,0,30)	$(\frac{1}{\sqrt{2}}, \frac{1}{\sqrt{2}}, 0)$	20
3	(30,30,30)	(0,1,0)	$\frac{20}{\sqrt{2}}$

of the experiment (figure 2). Signal to noise ratio of the simulated data is described by a reduced  $\chi^2$  (see figure 5). It was calculated as  $\chi^2(t) = \frac{1}{L} \sum_i b_i^2(t) = \frac{2}{L}$ , where  $b(t)$  is the simulated data,  $\sigma_i^2$  are sensor variances and  $L$  is the number of sensors.

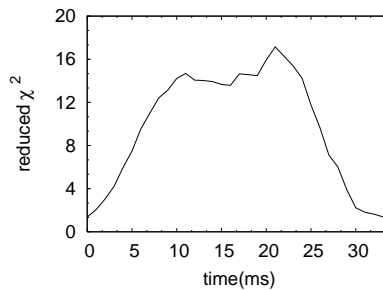


Fig. 5. Reduced  $\chi^2$  for the simulated data.

As stated earlier, there are many inverse algorithms that use the likelihood function. Rather than pick one such algorithm, we chose to summarize the effects each background model had on the function itself by numerically sampling the likelihood function using a dipole source model. To obtain this sampling we used a Monte Carlo Markov Chain (MCMC) approach [17]. The code used for sampling was developed in our group for Bayesian inference dipole analysis [4,18]. The number of dipoles was fixed at three. The free parameters for each dipole were the location, orientation and time course. The sampled dipole locations may be histogrammed to show the probability of reconstructed dipole locations in relation to the true dipoles. 1000 samples were generated for each covariance model and were used to summarize the likelihood in each case. Histograms of likelihoods of the distances between the true locations of dipoles and those obtained using different covariance models are in figure 6. They were constructed by histogramming the projection of the sampled dipole locations onto the line connecting the true dipole location and the mean location of the sampled dipoles. The origin of this line was set to the location of the true dipole. Only the results of the multi-pair covariance are consistent with the true locations for all three dipoles. Both the one pair and diagonal covariance models yielded inconsistent results, with that of the diagonal covariance being the most inconsistent.

In addition the width of the likelihood in the multi-pair case is wider than in the one pair or diagonal cases. We believe this is due to more positive correlation in the multi-pair case, which reduces the number of independent samples in the data and results in a wider distribution (eg. [19, p. 24]). To obtain additional support for this explanation we modeled the variances of the log likelihood function for each of these models. We calculate variance of the log likelihood (defined in (1)) around the true dipole location as:

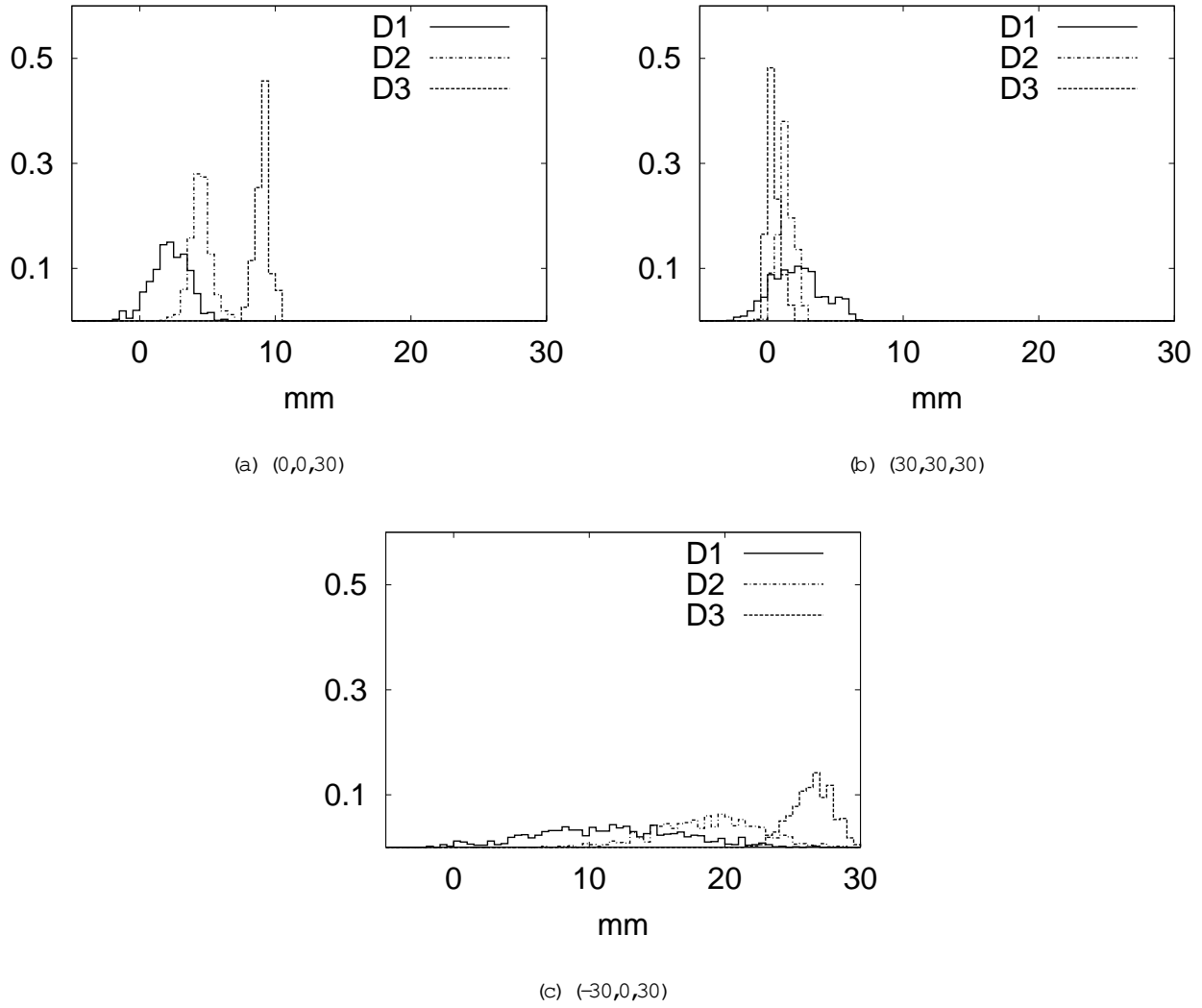


Fig. 6. Likelihoods of the distances between true locations of dipoles and those obtained using different covariance models. D 1 – multipair, D 2 – one pair estimated from the data, D 3 – diagonal.

$$E \left( \left[ (\mathbf{n}_0 + \sim)^T \quad \mathbf{1} (\mathbf{n}_0 + \sim) \quad E \left( (\mathbf{n}_0 + \sim)^T \quad \mathbf{1} (\mathbf{n}_0 + \sim) \right) \right]^2 \right):$$

Here  $\mathbf{n}_0$  is the noise from experimental data, and  $\sim$  is the white Gaussian noise. By using:

$$E \left( (\mathbf{n}_0 + \sim)^T \quad \mathbf{1} (\mathbf{n}_0 + \sim) \right) = \mathbf{n}_0^T \quad \mathbf{1} \mathbf{n}_0 + \text{Tr}(\quad \mathbf{1})$$

$$E \left( \sim^T \quad \mathbf{1} \sim^2 \right) = \text{Tr}(\quad \mathbf{1}^2) + \text{Tr}(\quad \mathbf{1})^2 + D \text{diag}(\quad \mathbf{1})^T \quad D \text{diag}(\quad \mathbf{1})$$

$$E \left( \mathbf{n}_0^T \quad \mathbf{1} \sim^2 \right) = \mathbf{n}_0^T \quad \mathbf{1} \sim^2;$$

we obtain:

$$E \left( \left[ (\mathbf{n}_0 + \sim)^T \quad \mathbf{1} (\mathbf{n}_0 + \sim) \quad E \left( (\mathbf{n}_0 + \sim)^T \quad \mathbf{1} (\mathbf{n}_0 + \sim) \right) \right]^2 \right) =$$

$$4\mathbf{n}_0^T \quad \mathbf{1} \sim^2 + \text{Tr}(\quad \mathbf{1})^2 + D \text{diag}(\quad \mathbf{1})^T \quad D \text{diag}(\quad \mathbf{1}):$$



$$\frac{\partial}{\partial (S^{-1})} = C S^T + \begin{matrix} & \begin{matrix} 2 & h & i & h & i & h & i & 3 \end{matrix} \\ \begin{matrix} 6 \\ 6 \\ 6 \\ 6 \\ 4 \end{matrix} & \begin{matrix} \text{tr}_h^T \ ^1F_{11_i} & \text{tr}_h^T \ ^1F_{12_i} & \dots & \text{tr}_h^T \ ^1F_{1T_i} \\ \text{tr}_T \ ^1F_{21} & \text{tr}_T \ ^1F_{22} & \dots & \text{tr}_T \ ^1F_{2T} \\ \vdots & \vdots & \ddots & \vdots \\ \text{tr}_T \ ^1F_{T1} & \text{tr}_T \ ^1F_{T2} & \dots & \text{tr}_T \ ^1F_{TT} \end{matrix} \end{matrix} :$$

Here,  $F_{ij}$  is an  $L \times L$  matrix obtained by splitting the full spatiotemporal covariance. It is an  $(i;j)^{\text{th}}$   $L \times L$  block in the  $CL \times CL$  matrix.  $F_{ij}$  is a  $C \times C$  matrix which is a block in  $LC \times LC$  matrix. It is constructed from the full spatiotemporal covariance. The  $(i;j)^{\text{th}}$  block matrix is obtained from nodes of a square grid with the upper left corner at  $(i-L; j-L)$  and the window size  $L \times L$ .  $L$  denotes the number of sensors and  $C$  denotes the number of time points used for analysis.

Having analytical derivatives, solutions can be obtained quickly with iterative algorithms. In this paper, we have used a fixed point method formulated as follows:

$$T_{k+1}^T = \frac{1}{L} \sum_{i,j} S_{kij} F_{ji}$$

$$S_{k+1}^T = \frac{1}{C} \sum_{i,j} T_{kij} F_{ji}$$

where  $k$  is the iteration number,  $T_{kij}$  and  $S_{kij}$  are elements of the inverted matrices  $T$  and  $S$ , respectively. Initial conditions for both matrices in our analysis were set to identity, which gave fast convergence.

### B. Validating estimation of one pair model

In order to show that the method we use for the estimation of the one Kronecker product model is valid, we start from an assumption that the noise was generated by such a model:

$$n = T^{\frac{1}{2}} S^{\frac{1}{2}} \sim;$$

where  $\sim$  is a column vector of white Gaussian noise of length  $LC$  and  $n$  is the resulting vector of correlated Gaussian noise. This can be represented in another form if we generate Gaussian noise in the form of an  $L \times C$  matrix, where  $L$  is the number of sensors and  $C$  - number of time points:

$$n = S^{\frac{1}{2}} T^{\frac{1}{2}};$$

with  $n$  being the resultant  $L \times C$  correlated Gaussian noise sample. In section B spatial and temporal covariances were estimated as

$$S = E n n^T$$

$$T = E n^T n :$$

If we use the above formulation of  $n$  this simplifies to the following

$$S = S^{\frac{1}{2}} \text{Trace}(T) S^{\frac{1}{2}} = \text{Trace}(T) S$$

$$T = \text{Trace}(S) T :$$

With normalization we get

$$\frac{\mathbf{T}^{-1} \mathbf{S}}{\text{Trace}(\mathbf{T}^{-1} \mathbf{S})} = \mathbf{T}^{-1} \mathbf{S}:$$

Thus, for the noise that has spatiotemporal covariance structure described by a Kronecker product both spatial and temporal covariances could be recovered by the procedure described in (10) up to a multiplicative constant. The constant is not important since we are able to demonstrate validity of the approach without calculating it.

#### Acknowledgements

This work was supported by the Mental Illness and Neuroscience Discovery Institute, and NIH grant 2 R01 EB000310-05. We thank Daniel Sheltraw for help with conducting the empirical MEG experiment at the Albuquerque VA Medical Center and for help using the hard-real-time stimulation software, RT Stim (<http://www.unm.edu/~sheltraw/rtstim/>). We thank Elaine Best for help in pre-processing the empirical data using MEGAN (<http://www.lanl.gov/p/p21/megan.shtml>). Figures showing the results of the Bayesian dipole analysis were generated using MRVIEW (<http://www.lanl.gov/p/p21/mrview.shtml>).

#### References

- [1] H. M. Huizenga, J. C. De Munck, L. J. Waldorp, and R. P. G rasman, "Spatiotemporal EEG/MEG source analysis based on a parametric noise covariance model," *IEEE Trans Biomed. Engin.*, vol. 50, pp. 533{539, 2002.
- [2] M. Hamalainen, R. Hari, R. J. Ilmoniemi, J. Knuutila, and O. V. Lounasmaa, "Magnetoencephalography: theory, instrumentation, and applications to noninvasive studies of the working human brain," *Rev. Mod. Phys.*, vol. 65, pp. 413{497, 1993.
- [3] S. Baillet, J. J. Riera, G. Marin, J. F. Mangin, J. Aubert, and L. Gamero, "Evaluation of inverse methods and head models for eeg source localization using a human skull phantom," *Phys. Med. Biol.*, vol. 46, pp. 77{96, 2001.
- [4] D. M. Schmidt, J. S. George, and C. C. Wood, "Bayesian inference applied to the electromagnetic inverse problem," *Human Brain Mapping*, vol. 7, pp. 195{212, 1999.
- [5] J. W. Phillips, R. M. Leahy, and J. C. Mosher, "MEG-based imaging of focal neuronal current sources," *IEEE Trans. Med. Imag.*, vol. 16, pp. 338{348, 1997.
- [6] S. E. Robinson and J. Vrba, "Functional neuroimaging by synthetic aperture magnetometry (SAM). Sendai: Tohoku University Press,, 1999, pp. 302{305.
- [7] Hamalainen M S and Ilmoniemi R J., "Interpreting magnetic fields of the brain: minimum norm estimates." *Med Biol Eng Comput*, vol. 32, no. 1, pp. 35{42, Jan. 1994.
- [8] S. Kuriki, F. Takeuchi, and T. Kobayashi, "Characteristics of the background fields in multichannel-recorded magnetic field responses." *Electroencephalography and clinical neurophysiology evoked potentials*, vol. 92, pp. 56{63, 1994.
- [9] H. Huizenga and P. Molenaar, "Ordinary least squares dipole localization is influenced by the reference," *Electroencephalography and clinical neurophysiology*, vol. 99, pp. 562{567, 1996.
- [10] B. Lutkenhoner, "Dipole source localization by means of maximum likelihood estimation. II. Experimental evaluation." *Electroencephalogr Clin Neurophysiol*, vol. 106, no. 4, pp. 322{9, 1998. [Online]. Available: <http://utils.ncbi.nlm.nih.gov/entrez/utils/elink.fcgi?cmd=prlinksn&db%from=pubmedn&retmode=refn&id=9741760>

- [1] S. C. Jun, B. A. Pearlmutter, and G. Nolte, "Fast accurate MEG source localization using a multilayer perceptron trained with real brain noise," *Physics in Medicine and Biology*, vol. 47, no. 14, pp. 2547{2560, July 21 2002.
- [2] V. Strassen, "Gaussian elimination is not optimal," *Numerische Mathematik*, vol. 13, no. 4, p. 354, 1969.
- [3] D. Coppersmith and S. Winograd, "Matrix multiplication via arithmetic progressions," *Journal of Symbolic Computation*, vol. 9, no. 3, pp. 251{80, March 1990.
- [4] J. C. De Munck, H. M. Huizenga, L. J. Waldorp, and R. Heethaar, "Estimating stationary dipoles from MEG/EEG data contaminated with spatially and temporally correlated background noise," *IEEE Trans Biomed. Engin.*, vol. 50, pp. 1565{1572, 2002.
- [5] M. W. Browne and G. Arminger, *Specification and estimation of mean- and covariance-structure models*. New York: Plenum, 1995.
- [6] A. Ahonen, M. Hamalainen, M. Kajola, J. Knuutila, P. Laine, O. Lounasmaa, L. Parkkonen, J. Simola, and C. Tesche, "122-channel SQUID instrument for investigating the magnetic signals from the human brain," *Physica scripta*, vol. T 49A, pp. 198{205, 1993.
- [7] A. Gelman, J. B. Carlin, H. S. Stern, and D. B. Rubin, *Bayesian Data Analysis*. London: Chapman & Hall, 1995.
- [8] S. Jun, J. George, J. Pare-Blagoev, S. Plis, D. Ranken, D. M. Schmidt, and C. Wood, "Dipole analysis on spatiotemporal MEG signals using bayesian inference," *Brain Topography*, vol. 16, p. 186, Nov. 19{23 2004. [Online]. Available: <http://hsc.unm.edu/som/cobre/isbet2003/>
- [9] W. T. Eadie, D. Drijard, F. E. James, M. Ross, and B. Sadoulet, *Statistical Methods in Experimental Physics*. Amsterdam: North Holland Publishing Company, 1971.